Hydrodynamics of Horseradish Peroxidase Revealed by Global Analysis of Multiple Fluorescence Probes

Juan E. Brunet,* Victor Vargas,‡ Enrico Gratton,§ and David M. Jameson¶

*Instituto de Química, Universidad Católica de Valparaiso, Valparaiso, Chile; ‡Departamento de Química, Facultad de Ciencias, Universidad de Chile, Santiago, Chile; §Department of Physics, Laboratory for Fluorescence Dynamics, University of Illinois at Urbana-Champaign, Urbana, Illinois, USA; and ¶Department of Biochemistry and Biophysics, University of Hawaii, Honolulu, Hawaii, USA

ABSTRACT Previous fluorescence studies of horseradish peroxidase conjugated with protoporphyrin IX suggested that the protein behaved hydrodynamically as a prolate ellipsoid of axial ratio 3 to 1. The present study, designed to further investigate the hydrodynamics of this protein, exploits a series of probes, noncovalently bound to the heme binding site of apohorseradish peroxidase, having different orientations of the excitation and emission transition dipoles with respect to the protein's rotational axes. The probes utilized included protoporphyrin IX and the naphthalene probes 1-anilino-8-naphthalene sulfonate, 2-*p*-toluidinyl-6-naphthalene sulfonate, and 4,4′-bis(1-anilino-8-naphthalene sulfonate). Time-resolved data were obtained using multifrequency phase fluorometry. The global analysis approach to the determination of molecular shape using multiple probes was evaluated by utilizing all data sets while maintaining a constant molecular shape for the protein. The results indicated that, in such analyses, probes exhibiting a single exponential decay and limited local motion have the major weight in the evaluation of the axial ratio. Probes that show complex decay patterns and local motions, such as the naphthalene derivatives, give rise to significant uncertainties in such global treatments. By explicitly accounting for the effect of such local motion, however, the shape of the protein can be reliably recovered.

INTRODUCTION

Horseradish peroxidase (donor: hydrogen-peroxidase oxidoreductase, EC 1.11.1.7) (HRP) is a heme protein that catalyzes the oxidation and peroxidation of a variety of organic and inorganic compounds. HRP, a glycoprotein of molecular mass 44,000 Da (approximately 18% of the molecular mass is due to eight covalently linked carbohydrate chains), contains one noncovalently bound hemin moiety. Although the sequence of the HRP-C isoenzyme has been elucidated (Welinder, 1976, 1979, 1985) and the protein has recently been cloned (Smith et al., 1990), crystal structures have not yet been obtained.

Early hydrodynamic studies on HRP using sedimentation velocity and diffusion experiments indicated a nonspherical protein with a frictional coefficient ratio (f/f_o) of 1.36 (Cecil and Ogston, 1951). Fluorescence methods can also provide information pertaining to average protein shapes in solution (Weber, 1952, 1966; Tao, 1969; Jameson and Hazlett, 1991). Early time-resolved fluorescence depolarization measurements on an apohorseradish peroxidase/1-anilino-8-naphthalene sulfonate complex were, however, inconclusive regarding the geometry of the macromolecule (Tao, 1969). More recent time-resolved measurements on an apohorseradish peroxidase-protoporphyrin IX adduct, though, indicated a nonspherical protein (Jullian et al., 1989); these data were consistent with a prolate ellipsoid of axial ratio near 3.

In the case of spherical proteins, analysis of the anisotropy decay of a single probe-protein complex is sufficient to determine the hydrodynamic aspect. For an anisotropic rotor, measurement of the steady-state anisotropy at a single excitation wavelength can provide information on the average rotational rate, which can then be compared with the rate of rotation of a sphere of equivalent molecular volume; from this comparison one can infer the degree of elongation. More information can be obtained exploiting different excitation wavelengths, which results in variation of the relative orientation of the excitation and emission dipoles (Weber, 1983; Barkley et al., 1981). However, to make full use of this approach the exact orientation of the dipole transitions with respect to protein axes must be known.

Brand and co-workers (Beechem et al., 1986) suggested that detailed hydrodynamic information for macromolecules can be realized by obtaining time-resolved data on multiple fluorescence probes and by analyzing these data using global analysis procedures. Using this approach some characteristics of the molecular shape can be held invariant among data sets obtained using different probes. Specifically, Brand and co-workers (Beechem et al., 1986) discussed the evaluation of multiple probe data sets in hydrodynamic studies on horse liver alcohol dehydrogenase. They found that, although the simple exponential analysis using a single rotational component provided reasonable data fits, the values of the rotational correlation times recovered varied considerably depending upon the probe utilized. Instead, a global analysis of all data sets allowed them to assign two rotational correlation times to the protein.

In this report we elaborate on the Brand method and describe an experimental study using the global analysis approach carried out on several apohorseradish peroxidase-fluorophore complexes, with the goal of obtaining information on the average protein shape. Our time-resolved studies were on apohorseradish peroxidase complexed with four

Received for publication 20 July 1992 and in final form 25 October 1993.

Address reprint requests to Dr. Juan E. Brunet, Instituto de Química, Universidad Catolica de Valparaiso, Casilla 4059 Valparaiso, Chile.

0006-3495/93/02/446/08 $2.00

fluorescence probes: protoporphyrin IX (PPIX), 1-anilino-8-naphthalene sulfonate (1,8-ANS), 4,4′-bis(1-anilino-8-naphthalene sulfonate) (bis-ANS) and 2-*p*-toluidinyl-6-naphthalene sulfonate (2,6-TNS). The naphthalene-based probes were chosen for their relatively long lifetimes, high affinity for the hemin binding site, and (in the case of 1,8-ANS and 2,6-TNS) their high polarization values at the exciting wavelength, indicating quasi-colinearity between absorption and emission transition dipole moments. The purpose of using these different probes was to selectively view rotational motions about different axes of the protein, which then appear as different diffusional constants in the analysis of anisotropy decay data. The basis of the method is the simultaneous analysis of the time-resolved depolarization data by imposing the same protein shape for all probe-protein complexes while leaving the orientational details of each probe, with respect to the protein major axis, free to vary. This type of target analysis can be readily implemented using global analysis procedures (Beechem et al., 1989). The target analysis can be further constrained using the known value of r_0, the initial anisotropy of each probe, and by imposing an average rotational correlation time determined by the known molecular weight of the protein.

THEORETICAL BACKGROUND

We shall first review the theoretical background for the description of anisotropic rotations and then demonstrate how the theory allows for the separation of macromolecular shape from the orientational details of the probes.

Anisotropic rotations

The basic equation for the time-dependent fluorescence anisotropy $r(t)$ of a fluorescent molecule rigidly attached to a protein, modeled as an ellipsoid of revolution, is a sum of three exponential terms (Tao, 1969; Favro, 1960; Wahl and Weber, 1967; Weber, 1971; Bedford et al., 1972; Chuang and Eisenthal, 1972; Ehrenberg and Rigler, 1972). Experimental determination of the fluorescent lifetimes (τ), the pre-exponential factors (β), and correlation times (Φ) for the probe-protein complexes allows us to evaluate the hydrodynamic parameters.

$$r(t) = \sum_{J=1}^{3} \beta_J e^{-\tau/\Phi_J} \tag{1}$$

with

$$\beta_1 = 0.1(3\cos^2\theta a - 1)(3\cos^2\theta e - 1) \tag{2}$$

$$\beta_2 = 0.3\sin^2\theta a \sin^2\theta e \cos 2\theta ae \tag{3}$$

$$\beta_3 = 1.2\sin\theta a \cos\theta a \sin\theta e \cos\theta e \cos\theta ae \tag{4}$$

where the angles θa, θe, and θae represent the angle between the absorption oscillator and the symmetry axis, the angle between the emission oscillator and the symmetry axis, and the angle between the projections of the absorption and emission oscillators onto the equatorial plane, respectively (Fig. 1, *top*).

The rotational correlation times are given by

$$\Phi_1 = (6D_\perp)^{-1} \tag{5}$$

$$\Phi_2 = (2D_\perp + 4D_\parallel)^{-1} \tag{6}$$

$$\Phi_3 = (5D_\perp + D_\parallel)^{-1} \tag{7}$$

The diffusion coefficients for symmetrical ellipsoids of revolution are

$$D_\perp = \tfrac{3}{2}D_s\mu\{(2\mu^2 - 1)S - \mu\}/(\mu^4 - 1) \tag{8}$$

$$D_\parallel = \tfrac{3}{2}D_s\mu(\mu - S)/(\mu^2 - 1) \tag{9}$$

where μ is the axial ratio and D_s is the diffusion coefficient for a sphere of equivalent volume V, which can be equated by the Debye-Stokes-Einstein relation to the rotational

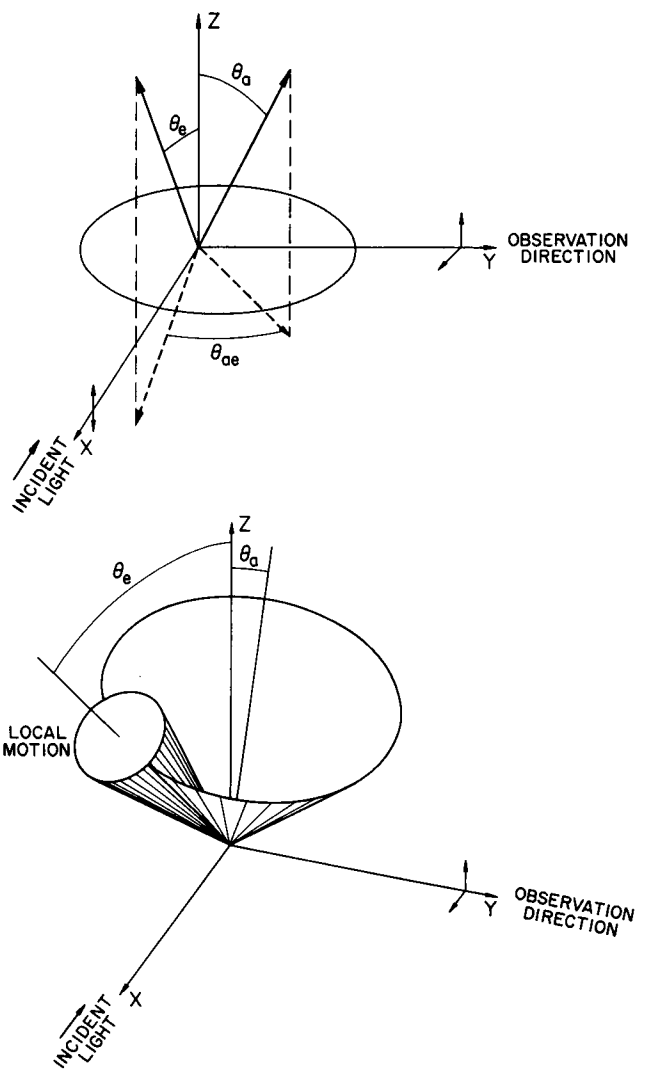

FIGURE 1 *Top*: schematic representation defining the angles θe, θa, and θae with respect to the direction of excitation, the direction of observation, and the rotational axes of the macromolecule. *Bottom*: addition of a local motion, defined by the angle Ψ.

diffusion coefficient:

$$D_s = kT/6\eta V \quad (10)$$

where η is the viscosity, k the Boltzmann constant, and T the absolute temperature. For an oblate rotor μ is less than 1, while for a prolate rotor μ is greater than 1; S is then given by

$$S_{(\text{oblate})} = [1/\sqrt{1-\mu^2}]\tan^{-1}[\sqrt{1-\mu^2}/\mu] \quad (11)$$

$$S_{(\text{prolate})} = [1/\sqrt{\mu^2-1}]\ln[\mu + \sqrt{\mu^2-1}] \quad (12)$$

An ellipsoid of revolution may be characterized by three rotational rates but only two diffusional constants: $D_\parallel$ and $D_\perp$. Experimentally these three rotational rates are difficult to obtain individually since they may differ very little from one another, and the lifetime of the probes are often short as compared with the correlation times.

We note that in the case of an ellipsoid of revolution the rotational correlation times are independent of the orientational details of the absorption and emission dipoles of the probe with respect to the protein's axes (Eqs. 5–7). We also note that Φ_3 is very close to Φ_1 if $D_\perp$ is much larger than $D_\parallel$. The pre-exponential factors (Eqs. 2–4) depend only on the relative orientation of the absorption and emission dipoles, with respect to the diffusional axes, and not on the shape of the protein. In particular, for probes with quasi-colinear absorption and emission dipoles, such as 1,8-ANS and 2,6-TNS, the expressions for the pre-exponential factors depend only on one angle, θa, and simplify to

$$\beta_1 = 0.1(3\cos^2\theta a - 1)^2 \quad (13)$$

$$\beta_2 = 0.3\sin^4\theta a \quad (14)$$

$$\beta_3 = 1.2\sin^2\theta a\cos^2\theta a \quad (15)$$

In one limiting case, where θa equals zero (that is the absorption and emission dipoles are aligned along the symmetry axis of the protein), then $\beta_1 = 0.4$ and $\beta_2 = \beta_3 = 0$, and only one diffusion coefficient, $D_\perp$, can be measured. When the projection of the absorption and emission dipoles on the equatorial plane is 90°, then the pre-exponential factors reduce to

$$\beta_1 = 0.1(3\cos^2\theta a - 1)(3\cos^2\theta e - 1) \quad (16)$$

$$\beta_2 = -0.3\sin^2\theta a\sin^2\theta e \quad (17)$$

$$\beta_3 = 0 \quad (18)$$

One then notes that orientations of the absorption and emission dipoles exist that will give rise to negative pre-exponential values.

For probes with noncolinear absorption and emission dipoles, such as PPIX and, in the case of the excitation wavelength utilized, bis-ANS, such simplifications of the pre-exponential expressions cannot apply. Since our final goal was to determine the hydrodynamic aspect of the protein, the analysis of the anisotropy decay data was carried out by imposing the protein's shape in all data sets. This approach implies that the rotational correlation times are independent of the probe utilized. The pre-exponential factors can instead be different for the various probes. The global analysis method has been specifically designed to allow some fitting parameters such as the correlation times to be the same for all data sets, while other parameters such as the orientation of the probe may vary among the data sets.

The basic equations, however, all assume that the probe molecule is rigidly attached to the protein and experiences no local rotational motion, whether due to libration of the probe or to internal protein motion (e.g., due to a domain structure). If such local motions or an excited state process exists that gives rise to an additional depolarization, then the equations given above are not strictly valid. We found that in order to account for a local motion of the probe, it is necessary to change the angular variables in terms of r_0, the initial anisotropy, the absorption transition angle, θa, and the local motion, Ψ, with respect to the azimuthal angle as shown in Fig. 1 (*bottom*). For any given absorption transition angle, the initial anisotropy value, r_0, constrains the emission transition dipole angle to lie on the surface of a cone of semiangle determined by r_0 and angle Ψ determined by the particular orientation of the probe with respect to the protein principal axis. In Fig. 1 (*bottom*) the x- and y-axes are equivalent given the hypothesis of an ellipsoid of rotation. The local motion of the probe then appears as an additional diffusive cone around the equilibrium position. To account for local motion we assume that r_0 rapidly relaxes to a value of r_∞ with an exponential relaxation time ϕ_L. The program introduces two additional parameters $r_d = (r_0 - r_\infty)$ and ϕ_L. In the absence of isotropic local motion $r_d = 0$. On the basis of the experimental results we will discuss for each particular situation the effect of probe local motion.

MATERIALS AND METHODS

Preparation of HRP conjugates

1,8-ANS, bis-ANS, and 2,6-TNS (Molecular Probes) were used without further purification. Horseradish peroxidase type VI was from Sigma. The heme group was removed using Teale's method of cold acid and butanone extraction (Teale, 1959) followed by exhaustive dialysis at 4°C against 0.1 M sodium phosphate buffer (pH 7.4). The concentration of apoHRP was determined spectrophotometrically using a molar absorption coefficient at 280 nm of 20,000 (Tamura et al., 1971). The apoHRP conjugates with the naphthalene derivatives were prepared in phosphate buffer (0.1 M, pH 7.4) with at least a 20-fold molar excess of protein to rule out contribution from free probe. The stoichiometry of the protein-probe conjugates was measured by hemin titration following the heme absorption and the reduction of the probe fluorescence (Vargas et al., 1990). In all the conjugates a 1:1 stoichiometry was found.

Fluorescence time-resolved measurements

Lifetime and dynamic polarization measurements were carried out using either an ISS Greg 200 spectrofluorometer or a home-built multifrequency phase and modulation fluorometer (Gratton and Limkeman, 1983). Excitation of the HRP conjugates was accomplished using either the 514.5 nm or the 363.8 nm line of an argon ion laser (Spectra-Physics model 2035-3.5S) for the PPIX or naphthalene probes, respectively. The respective emissions

were observed through a Schott OG 570 cuton filter (which passes wavelengths longer than 550 nm) or a Schott KV399 cuton filter (which passes wavelengths above 380 nm). For lifetime measurements the exciting light was polarized parallel to the vertical laboratory axis, while the emission was viewed through a polarizer oriented at 55°. In the multifrequency phase and modulation technique the intensity of the exciting light is modulated, and the phase shift and relative modulation of the emitted light, with respect to the excitation, are determined (Spencer and Weber, 1969). Phase and modulation lifetimes are then calculated according to the known equations (Spencer and Weber, 1969; Jameson et al., 1984; Gratton et al., 1984). Differential phase and modulation data were analyzed using the Globals Unlimited program with modifications to allow direct fitting of the axial ratio, the average diffusional rate D_s and the local motion of the probe determined by r_d and ϕ_L. In the nonlinear least-squares approach, the goodness of fit of the measured phase and modulation data to a particular model is judged by the value of the reduced χ^2 (Jameson et al., 1984).

RESULTS

The intensity decay multifrequency phase and modulation data on the HRP conjugates are shown in Fig. 2. The naphthalene derivatives show heterogeneous decays, while the PPIX conjugate decays monoexponentially. The results of discrete exponential decay analyses are given in Table 1.

The nonexponentiality of the intensity decay poses a problem in the association of lifetime values with rotational species. In the following we have assumed a nonassociative model, that is, one in which the measured lifetime heterogeneity reflects details of the interaction of the probe with the protein matrix rather than a microheterogenity in the protein population per se.

TABLE 1 Two-component lifetimes and fractional intensities of HRP conjugates in phosphate buffer (0.1 M, pH 7.4) at 20°C

Probe	τ_1	f_1	τ_2	f_2	χ^2
PPIX	16.86	1.000	—	—	1.28
1,8-ANS	18.48	.926	4.42	.074	0.75
2,6-TNS	10.31	.896	2.15	.104	4.37
bis-ANS	9.94	.690	4.16	.310	3.87

τ_1, τ_2, lifetimes in nanoseconds.
f_1, f_2, fractional intensities.
χ^2, reduced chi-square; calculated using 0.2° and 0.004 for phase and modulation SD, respectively.

The dynamic polarization data (phase and modulation ratio values) are shown in Fig. 3. Inspection of this figure shows that the maxima of the curves occur in different frequency regions, which implies that the probes sense different rotational aspects of the protein since the differences in the lifetime values are not large enough to affect the positions of these maxima greatly. Also we note that none of the probes show extensive local motion as evidenced by the downward curvatures at higher modulation frequencies and the interception of the AC modulation ($I_\perp/I_\parallel$) data on the high-frequency vertical axis at values close to the known r_o values.

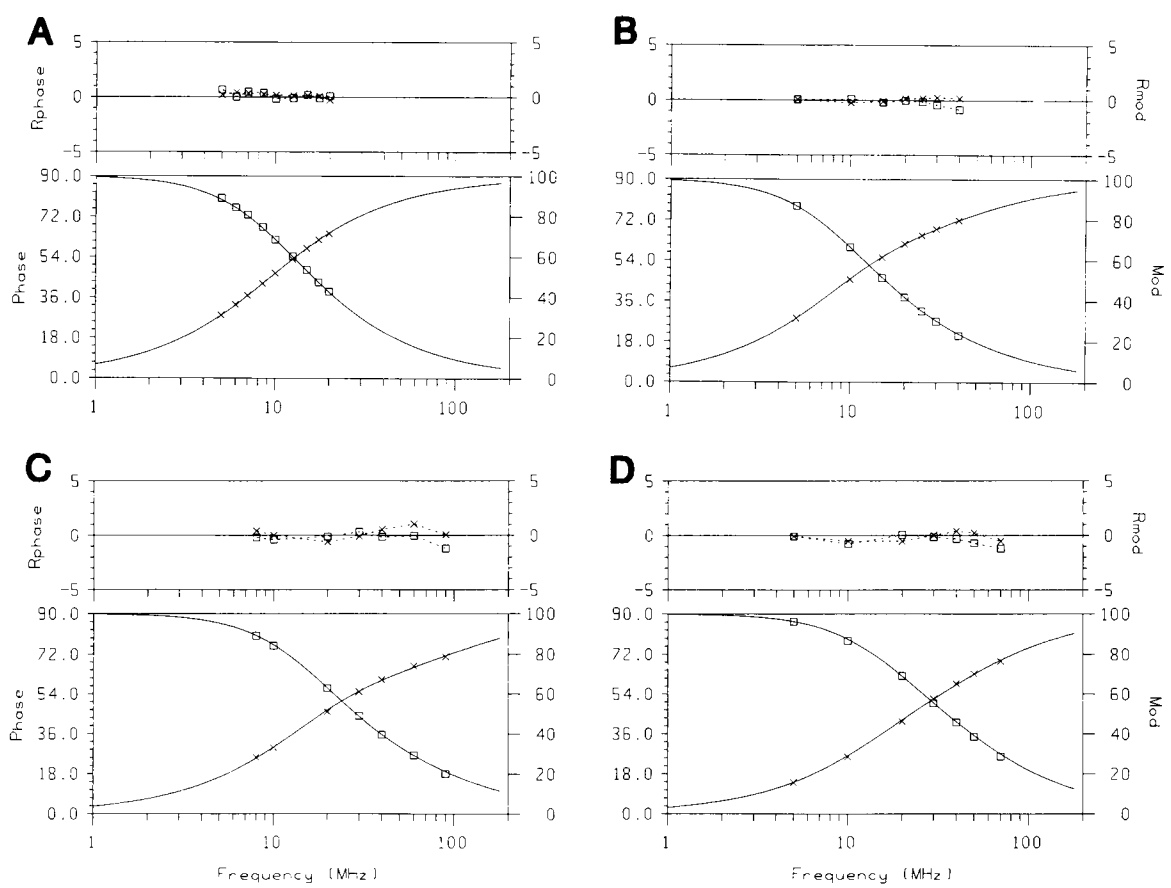

FIGURE 2 Phase (×) and modulation (□) lifetime data on PPIX/HRP (*A*), ANS/HRP (*B*), TNS/HRP (*C*), and bis-ANS/HRP (*D*). The solid lines correspond to the decay schemes given in Table 1. The *R* phase values are the residues based on the fit to the indicated decay scheme.

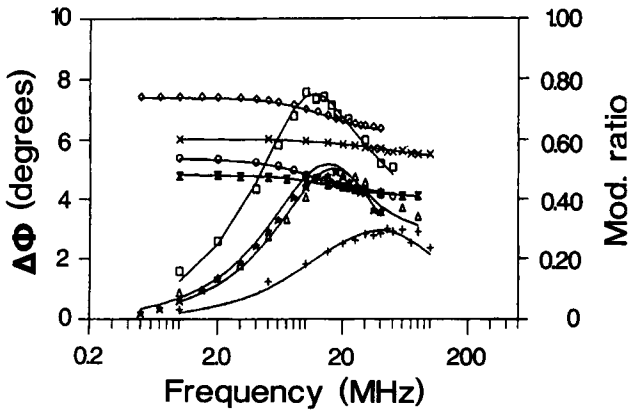

FIGURE 3 Dynamic polarization data for the four HRP adducts. Phase and modulation results for PPIX/HRP (★, ◇), ANS/HRP (□, ○), TNS/HRP (△, ⧖), and bis-ANS/HRP (+, ×). Solid lines correspond to the calculated curves for the parameters given in Table 3.

We should emphasize that these observations are performed on the rough data and are independent of the models we will use for the rotational analysis. These observations are thus analogous to the initial calculations of Brand and co-workers (Beechem et al., 1986) on the average rotational correlation times seen by the various probe/protein complexes. However, as we will discuss later, the local motions displayed by the anilinonaphthalene probes, though apparently not extensive, are sufficient to significantly complicate the analysis of the protein's shape.

The target analysis approach requires that the fit be performed using only two parameters for the hydrodynamic shape, either ($D_{\|}$, $D_{\perp}$) (D_s, μ). These are the parameters that must be linked during the analysis since they depend only on the molecular shape and not on the details of the probe orientation.

Analysis using D_s and μ

If we analyze only the PPIX results we find an axial ratio value of 3.4 (consistent with the previous study, Jullian et al., 1989). However, analysis of all data sets gives the results reported in Table 2. Inspection of this table suggests that the apparent shape of the molecule is oblate, i.e., μ is less than unity. The question then arises as to why inclusion of the data on the naphthalene probes results in such a different shape for the protein than does the analysis obtained using only the PPIX data. What we believe is happening is that among the four data sets the PPIX adduct can fit almost as well as for a prolate as for an oblate ellipsoid. This result can be due to a particular orientation of the probe in the macromolecule that senses primarily one of the rotational motions. Instead, the major weight in determining the oblate shape in the global analysis can come from the three naphthalene probes that, due to their local motion, can cause one molecular axis to appear to be faster than the others. To evaluate the extent of such local motion we then carried out a three exponential decay analysis.

TABLE 2 Global analysis of dynamic polarization data (D_s and μ linked)

Probe	$1/D_s$	μ	θe	θa	θae	χ^2
PPIX	188	0.388	32.9	32.9	74.0	0.24
1,8-ANS	188	0.388	66.7	86.8	0	2.47
2,6-TNS	188	0.388	61.5	80.9	0	4.04
bis-ANS	188	0.388	0	33.2	88.4	3.50
Global χ^2 = 1.71						
13 free parameters						

θe, θa, θae, angles defined in Fig. 1 *A*.
$1/D_s$, reciprocal of the average diffusional rate constant in nanoseconds.
μ, axial ratio.
χ^2, reduced chi-square calculated using 0.2° and 0.004 for the phase and modulation SDs, respectively.

Sum of exponentials

The ellipsoid of rotation model gives three exponential times in the anisotropy decay. However, the three rotational correlation times are within a narrow range, and a local motion can appear as a term with a very different rotational correlation time. Therefore, the exponential analysis has the advantage that it can reveal the presence of local motions of the probe, which is not explicitly included in the model described by Eqs. 2–12. The existence of local motion is, in fact, indicated by the presence of a very short rotational correlation time in this analysis. The result of this analysis is shown in Table 3, which also shows a lower χ^2 value for this model. This lower χ^2 value is not very significant, though, when the number of free parameters for the models is taken into account. This analysis clearly indicates that the PPIX adduct displays only two rotational rates, with significant amplitudes, in the expected time range, while the naphthalene adducts show three such rotational rates, one of which is very short. The relative value of the pre-exponential factors of the short rotational correlation time component is on the order of 10% of the total amplitude. Furthermore, the second pre-exponential factors are negative. The question arises as to whether the hydrodynamic shape of the molecule can be recovered at all in the presence of this local motion. If this motion occurs along one of the molecular axes of the molecule, this axis may appear as a "fast rotational axis," and the hydrodynamic shape determined by the comparison of $D_{\|}$ and $D_{\perp}$ may be incorrectly obtained, which in fact happens.

Analysis with additional local motion

The analysis performed using an additional local motion for the probe is shown in Table 4. In this analysis the values of r_o for the different probes were set to the experimentally measured value for these probes in highly viscous solvents. Furthermore, the diffusional rate of the sphere of equivalent molecular mass was also fixed to 1/120 ns, using the approximation of 1 ns rotational correlation time per each 2400 Da of molecular mass ($1/D_s = 6\tau_c$). The value of the χ^2 obtained in this treatment is comparable to that obtained in the previous analysis, even though the number of parameters utilized for the fit were less. For this fit the recovered protein

TABLE 3 Global analysis of dynamic polarization data: sum of exponential (rotational correlation times are linked in this fit)

Probe	r_o	ϕ_1	β_1	ϕ_2	β_2	ϕ_3	β_3	χ^2
PPIX	0.167	36.2	0.402	23.2	0.595	2.3	0.003	0.201
1,8-ANS	0.343	36.2	1.314	23.2	−0.410	2.3	0.096	0.902
2,6-TNS	0.344	36.2	1.293	23.2	−0.390	2.3	0.097	0.590
bis-ANS	0.231	36.2	1.625	23.2	−0.797	2.3	0.172	0.599
Global χ^2 = 0.537								
19 free parameters								

ϕi, rotational correlation times in nanoseconds.
βi, pre-exponential factors.
r_o, time zero anisotropy.
χ^2, reduced chi-square calculated using 0.2° and 0.004 for the phase and modulation SDs, respectively.

TABLE 4 Global analysis of dynamic polarization data: additional local motion (D_s and μ linked)

Probe	$1/D_s$	μ	r_o	r_a	ϕ_1	θ_a	Ψ	χ^2
PPIX	120	2.80	0.167	0.001	0.000	75.44	128.0	0.217
1,8 ANS	120	2.80	0.335	0.079	4.500	0.00	0.0	0.950
2,6 TNS	120	2.80	0.352	0.097	1.185	0.00	0.0	0.678
bis-ANS	120	2.80	0.230	0.110	1.579	0.00	0.5	1.014
Global χ^2 = 0.654								
15 free parameters								

χ^2, reduced chi-square calculated using 0.2° and 0.004 for the phase and modulation SDs, respectively.
r_o, time zero anisotropy.
$1/D_s$, reciprocal of the average diffusional rate constant in nanoseconds.
ϕ_L, local correlation time in nanoseconds.
θa and Ψ, described in Fig. 1 *B*.
$r_d = r_o - r_\infty$.

shape is a prolate ellipsoid with an axial ratio of about 2.8. The χ^2 error surface using the rigorous error analysis method of the Global Unlimited software is shown in Fig. 4. Using this model the axial ratio is quite well determined. We note that if $1/D_s$ is variable then the evaluation of μ has much larger uncertainty.

DISCUSSION

Global analysis of the four HRP adducts has revealed that one of the adducts (PPIX) carries essentially all of the derived information on the prolate aspect of the protein, while the adducts with local motion gives an oblate apparent molecular

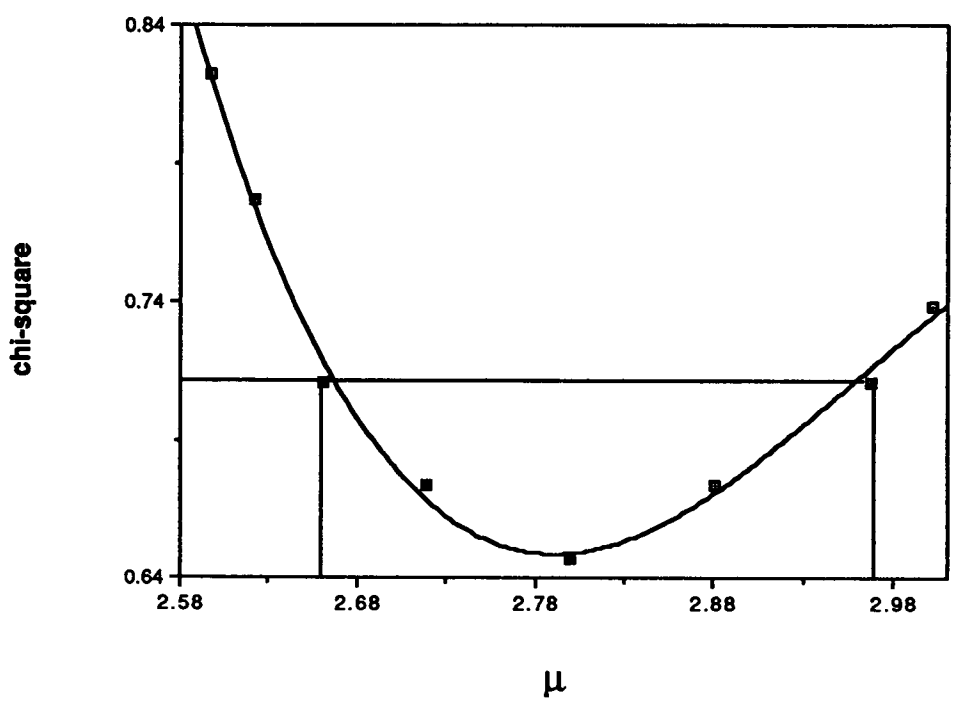

FIGURE 4 χ^2 error surface for the value of the axial ratio, μ. The vertical and horizontal lines indicate the values at one SD from the minimum χ^2 value.

shape if the local motion is not accounted for explicitly. We can conclude that for the multiple probe approach to be useful it is imperative that the probes either do not demonstrate significant local motion or that the extent of local motion is properly estimated. The three-exponential analysis, which is not a target analysis, provides a useful starting point since the results can be interpreted differently, depending on the values of the recovered rotational correlation times. The target analysis is very powerful if the "model" fits the data, otherwise it can provide misleading results if the only criterion to judge the fit is the global χ^2 and F-test. Instead, if a "physical constraint" is included, such as the fact that the molecule's shape cannot be very oblate, the model can be disregarded. We also note that the target analysis has provided similar probe orientations for the naphthalene probes, which can simply indicate that the three probes have local motions along the same probe axis.

The possibility of determining the axial ratio using the multiple probe approach critically depends on the amount of local motion and on the particular orientation of the probes with respect to the macromolecule. The analysis using three exponentials is useful in determining the extent of local motion. Even a small amount of local rotational freedom can appear as a fast rotational axis, which compromises the utility of using multiple probes. The data set on PPIX has the major weight in the determination of the axial ratio since at least one axis can be reliably determined. Therefore, the importance of using multiple probes must be reconsidered in light of the possibility of local motion and multiple lifetimes. For the multiple probe approach to properly succeed, it is important to have probes that are well anchored in the protein matrix. Also, the probe should be oriented at an appropriate angle with respect to the molecule axis, in order to determine more than one rotational diffusion rate. One may ask the question if explicit inclusion of local motions in these target analyses will significantly improve our ability to determine the proper hydrodynamic aspects. In fact, consideration of this possibility immediately brings to mind several levels of complexities, namely, (*a*) the assignment of associative versus nonassociative decays, (*b*) the possibility that for a given probe (for example PPIX) more than one orientation with the protein is allowed, and (*c*) degeneracy of the transition dipoles (in PPIX).

Another limitation of the method, in the presence of multiple exponential decay, is related to the association between decay constants and orientation of the probe with respect to the protein. If the probes can have different orientations in the heme binding site, which give rise to the lifetime heterogeneity, the equations used should include a distribution of orientations which we have not studied.

In conclusion, the multiple probe approach can, in principle, provide better accuracy for the determination of the axial ratio when compared with single probe determinations. However, the limit of applicability is determined by the availability of well-behaved probes.

This work was supported by National Science Foundation grants INT-8916623 and INT-930383 (DMJ and JEB) and DMB-9005195 (DMJ), FONDECYT-Chile grant 91-539 (JEB) and NIH grant RR03155-01 (EG).

REFERENCES

Barkley, M., A. A. Kowalczyk, and L. Brand. 1981. Fluorescence decay studies of anisotropic rotations of small molecules. *J. Chem. Phys.* 75: 3581–3593.

Bedford, G. G., R. I. Bedford, and G. Weber. 1972 Dynamics of fluorescence polarization of macromolecules. *Proc. Natl. Acad. Sci. USA.* 69: 1392–1393.

Beechem, J. M., E. Gratton, M. Amelot, J. R. Knutson, and L. Brand. 1989. The global analysis of fluorescence intensity and anisotropy decay data: second generation theory and programs. *In* Fluorescence Spectroscopy. Vol. 1. Principles and Techniques. J. R. Lakowicz, editor. Plenum Press, New York.

Beechem, J. M., J. R. Knutson, and L. Brand. 1986. Global analysis of multiple dye fluorescence anisotropy experiments on proteins. *Biochem. Soc. Trans.* 14:832–835.

Cecil, R., and A. G. Ogston. 1951. Determination of sedimentation and diffusion constants of horseradish peroxidase. *Biochem. J.* 49: 105–106.

Chuang, T. J., and K. B. Eisenthal. 1972. Theory of fluorescence depolarization by anisotropic rotational diffusion. *J. Chem. Phys.* 57: 5094–5098.

Ehrenberg, M., and R. Rigler. 1972. Polarized fluorescence and rotational brownian motion. *Chem. Phys. Lett.* 14:539–544.

Favro, L. D. 1960. Theory of the rotational brownian motion of a free rigid body. *Phys. Rev.* 119:53–62.

Gratton, E., D. M. Jameson, and R. D. Hall. 1984. Multifrequency phase and modulation fluorometry. *Annu. Rev. Bioeneg.* 13:105–124.

Gratton, E., and M. Limkeman. 1983. A continuously variable frequency cross-correlation phase fluorometer with picosecond resolution. *Biophys. J.* 44:315–324.

Jameson, D. M., E. Gratton, and R. D. Hall. 1984. The measurement and analysis of heterogeneous emissions by multifrequency phase and modulation fluorometry. *App. Spectrosc. Rev.* 20:55–105.

Jameson, D. M., and T. L. Hazlett. Time-resolved fluorescence in biology and biochemistry. *In* Biophysical and Biochemical Aspects of Fluorescence Spectroscopy. T. G. Dewey, editor. Plenum Press, New York. 105–133.

Jullian, C., J. E. Brunet, V. Thomas, and D. M. Jameson. 1989. Time-resolved fluorescence studies on protoporphyrin IX-apohorseradish peroxidase. *Biochim. Biophys. Acta.* 997:206–210.

Smith, A. T., N. Santama, M. Edwards, R. C. Bray, R. N. F. Thorneley, and J. F. Burke. 1990. Expression of a synthetic gene for horseradish peroxidase C in *Escherichia coli* and folding and activation of the recombinant enzyme with Ca^{2+} and heme. *J. Biol. Chem.* 265: 13335–13343.

Spencer, R. D., and G. Weber. 1969. Measurements of subnanosecond fluorescence lifetimes with a cross-correlation phase fluorometer. *Ann. N.Y. Acad. Sci.* 158:361–376.

Tamura, M., T. Asakura, and T. Yonetani. 1971. Heme modification studies on horseradish peroxidase. *Biochim. Biophys. Acta.* 268:292–304.

Tao, T. 1969. Time-dependent fluorescence depolarization and Brownian rotational diffusion coefficients of macromolecules. *Biopolymers.* 8: 609–632.

Teale, F. W. J. 1959. Cleavage of the haem-protein link by acid methylethylketone. *Biochim. Biophys. Acta.* 35:543.

Vargas, V., J. E. Brunet, and D. M. Jameson. 1990. Oxygen diffusion near the heme binding site of horseradish peroxidase. *Biochem. Biophys. Res. Commun.* 178:104–109.

Wahl, P., and G. Weber. 1967. Fluorescence depolarization of rabbit gamma globulin conjugates. *J. Mol. Biol.* 30:371–382.

Weber, G. 1952. Polarization of the fluorescence of macromolecules. I. Theory and experimental method. *Biochem. J.* 51:145–155.

Weber, G. Polarization of the fluorescence of solutions. *In* Fluorescence and

Phosphorescence Analysis. D. M. Hercules, editor. John Wiley and Sons, Inc., New York. 217–240.

Weber, G. 1983. Polarized fluorescence. *In* Fluorescence Techniques in Cell Biology. A. A. Thaer and M. Sternetz, editors. Springer-Verlag, New York. 5–13.

Weber, G. 1971. Theory of fluorescence depolarization by anisotropic Brownian rotations. Discontinuous distribution approach. *J. Chem. Phys.* 55:2399–2407.

Welinder, K. G. 1976. Covalent structure of the glycoprotein horseradish peroxidase (EC 1.11.1.7). *FEBS Lett.* 72:19–23.

Welinder, K. G. 1979. Amino acid sequence studies of horseradish peroxidase. *Eur. J. Biochem.* 95:483–502.

Welinder, K. G. 1985. Plant peroxidases. Their primary, secondary and tertiary structures and relation to cytochrome *c* peroxidase. *Eur. J. Biochem.* 151:497–504.